TRANSPORT
ISSN 1648-4142 print / ISSN 1648-3480 online
2014 Volume 29(1): 107–114
doi:10.3846/16484142.2013.789979

AN INVERSE DYNAMICS METHOD FOR RAILWAY VEHICLE SYSTEMS

Tao Zhu, Shoune Xiao, Guangwu Yang, Weihua Ma, Zhixin Zhang

State Key Laboratory of Traction Power, Southwest Jiaotong University, 610031 Chengdu, China

Submitted 17 May 2012; accepted 20 August 2012; first published online 22 May 2013

Abstract. The wheel–rail action will obviously be increased during the vehicles in high-speed operation state. However, in many practical cases, direct measurement of the wheel–rail contact forces cannot be performed with traditional procedures and transducers. An inverse mathematical dynamic model for the estimation of wheel–rail contact forces from measured accelerations was developed. The inverse model is a non-iteration recurrence method to identify the time history of input excitation based on the dynamic programming equation. Furthermore, the method overcomes the weakness of large fluctuations which exist in current inverse techniques. Based on the inverse dynamic model, a high-speed vehicle multibody model with twenty-seven Degree of Freedoms (DOFs) is established. With the measured responses as input, the inverse vehicle model can not only identify the responses in other parts of vehicle, but also identify the vertical and lateral wheel–rail forces respectively. Results from the inverse model were compared with experiment data. In a more complex operating condition, the inverse model was also compared with results from simulations calculated by SIMPACK.

Keywords: high-speed train, inverse dynamic model wheel–rail interaction, contact forces, identify response, railway.

Reference to this paper should be made as follows: Zhu, T.; Xiao, S.; Yang, G.; Ma, W.; Zhang, Z. 2014. An inverse dynamics method for railway vehicle systems, *Transport* 29(1): 107–114. http://dx.doi.org/10.3846/16484142.2013.789979

Introduction

Along with the rapid development of computer technology, satisfactory results can be obtained in large-scale simulation calculations of complex structures, such as finite element analysis and the multibody analysis. The precondition of using these methods is the determination of the load condition, because load will be used as inputs to get the system responses. However, due to the complexity of the structure and other environmental factors, in most of the cases it is difficult to directly measure the load. For example, the train is subjected to the wheel–rail impact loads when operating because of rail irregularities and crossing turnouts. Since the abovementioned loads play important roles in the safety of the structure, researchers can only apply the indirect method to obtain the overall load specification, thus the load identification method is developed (Zhu *et al.* 2011).

Currently, various methods for inverse identification problem associated with indirect force measurements have been proposed (Stevens 1987; Dobson, Rider 1990; Nordström, Nordberg 2002). Among them, two main methods are: the frequency domain (Giergiel, Uhl 1989a; 1989b) and the time domain method (Kammer 1998; Uhl, Pieczara 2003). Methods in the frequency domain require information about the Frequency Response Functions (FRF) of the investigated structures and the spectrum of responses measured during operation. Based on this information a spectrum of excitation forces can be estimated. Identification of the excitation forces can be formulated using the mutual-energy theorem proved by Heaviside in 1892 (Hansel 1991). These methods have been studying since early time, and have gained some success. And they have many advantages, such as simple dynamic calibration, high recognition accuracy, but require a certain length of signal samples, generally only applied to steady-state or stationary random dynamic load identification. Methods formulated in the time domain are mainly based on the relation between the excitation and system responses in the form of convolution. Developed in mid-1980s, these methods have been welcomed by the engineering community. Recently, due to intuitive use and user-friendliness, they have been rapidly developing.

Due to the complexity of the inverse identification problem in railway vehicle systems, not much research has been performed in this area. In China, the most current method is to periodically measure track irregularity with dedicated measurement vehicles. Several efforts ap-

Corresponding author Tao Zhu
E-mail: *232665368@qq.com*

pear in literature to predict vehicle reactions and wheel forces from measured track irregularity. Esveld (2001) reported an online vehicle response analysis system which had been developed using frequency response methods to estimate vehicle reactions from geometric irregularities. Direct measurement of track irregularity is expensive and restricted to specialized track measurement vehicles which measure at intervals that can exceed the time required for a track fault to develop.

There is a great need to formulate a method that can be based on measurement on the vehicle but not on the track. Using accelerometers mounted on the significant masses, accelerations can be measured inexpensively. If sufficient characteristics of the vehicle such as accelerations are known, it is possible to estimate the forces acting at the wheel–rail interface. Law *et al.* (1997) modeled the deck as a simply supported beam with a viscous damping parameter, and identified the contact forces by the measured bending moments and accelerations when the vehicle passed through a bridge with constant speed. The results were consistent with the experiment, however, this model became less accurate at high-frequency, at the same time its algorithm became more complexity and a longer computational time was needed (Law *et al.* 1997). Uhl and Pieczara (2003) proposed a genetic algorithm for the load estimation method, which was based on the measurements of system responses. This method can effectively validate the quasi-static characteristics of the vehicle effectively. Later Uhl (2007) proposed a new load estimation method for the wheel–rail force, since the study was carried out within the linear range, and there was a strong non-linear characteristics along the horizontal of the wheel–rail, a large deviation was found when contrasted to lateral force testing. Xia *et al.* (2008) developed an inverse wagon model which only employed the measurements of the wagon body responses as inputs to estimate the wheel–rail contact forces. Ronasi *et al.* (2009) identified the wheel–rail force as a non-linear least squares problem to solve the optimization problems, this was a rare instance of the use of non-linear load identification.

Above approaches require the computation of matrix inverse, and have a large calculation works. Some of these methods have poor numerical stability at the initial and end of load time history, and easily lead to an oscillation of the inverse force at these stages. The method that we propose in next section can overcome these shortcomings in some extent. In addition, as used to estimate the wheel–rail contact force for running vehicle, achieving the contact force identification in real-time is very important, it is basic requirements for online assessment the operating safety of the vehicle. It proposes much higher and more comprehensive requirements for the inversion method. Unfortunately, the current inverse methods can not be achieved.

Aim at the bottlenecks which encountered by the current inverse methods, this paper further explores an new inversion method. The wheel–rail contact forces can be identified in time domain using this method, and the other responses of the vehicle which not measured can also be reconstructed at the same time. The new method is based on the dynamic programming equations. The forces are identified in the time domain by a recursive formula, responses of the structure are also reconstructed by using the identified forces for comparison. The dynamic programming technique possess inherent limitations that cannot be avoided, however, the inverse technique inherently provides bounds to the ill-conditioned forces. Based on the inverse mathematical model, the inverse dynamic model for high-speed vehicle which has 27 degrees of freedom is established. Using the measured responses, the inverse vehicle model can not only identify the responses of the vehicle, but also identify the vertical and lateral wheel–rail forces respectively. The experiment and SIMPACK simulation study are compared with it.

1. Basis of Load Identification Theory

For a general finite element model of a linear elastic time-invariant structure, the dynamic governing equation is given by:

$$M\ddot{X}(t)+C\dot{X}(t)+KX(t)-F(t)=0\,, \tag{1}$$

where: M, C and K are the system mass, damping, and stiffness matrices, respectively; $\ddot{X}(t)$, $\dot{X}(t)$ and $X(t)$ are the acceleration, velocity and displacement vectors of the structure; F is the vector of the input excitation forces.

1.1. Discretization of Linear, Time-Variant Systems

Using the state space formulation, Eq. (1) is converted into a set of first order differential equations as follows:

$$\dot{x}=Ax+Bf\,, \tag{2}$$

where:

$$x=\begin{bmatrix}X\\ \dot{X}\end{bmatrix}_{2n\times 1};$$

$$A=\begin{bmatrix}0 & I\\ -M^{-1}K & -M^{-1}C\end{bmatrix}_{2n\times 2n};$$

$$B=\begin{bmatrix}0\\ M^{-1}f\end{bmatrix}_{2n\times 1},$$

where: x represents a vector of state variables of length $2n$, which contains the displacement and velocities.

For the load identification problem, the known responses of the system M, C and K are used to solve the unknown input vector $f(s)$ which is in discrete form. In order to facilitate the computer solution, these differential equations are then rewritten as discrete equations using the standard exponential matrix representation:

$$x_{i+1}=Sx_i+Df_i\,; \tag{3}$$

$$y_i=Qx_i\,, \tag{4}$$

where: $S=e^{Ah}$ is the exponential matrix, and together with matrix $D=A^{-1}(S-I)$ is the input influence matrix which represents the dynamics of the system and associ-

ates with load; Q is an $m \times 2n$ selection matrix relating the measurements to the state variables; x_{i+1} denotes the values at the $(i+1)$th time step of computations.

1.2. Statement Problem

In practice, it is not possible to measure all the displacements, velocities and accelerations, and only certain combinations of the variables x_i are measured. The goal is to find the forcing term f that causes the system described in Eq. (3) to best match the measurement. The least-squares error is now expressed as:

$$E = \sum_{i=1}^{N} \left(y_i - \hat{y}_i \right)^T \lambda_1 \left(y_i - \hat{y}_i \right), \tag{5}$$

where: T is the transpose of a matrix; y_i and $\hat{y}_i$ are the output variables of the system from the identification formula and measurement, respectively.

In most cases, all of the measurements are, in some degree, influenced by noise, called ill-problem, which should be avoided by adding a smoothing term to the least-squares error to become a non-linear least-squares problem:

$$E = \sum_{i=1}^{N} \left(y_i - \hat{y}_i \right)^T \lambda_1 \left(y_i - \hat{y}_i \right) + \left(f_i \right)^T \lambda_2 \left(f_i \right). \tag{6}$$

The second term is known as the regularization parameter and the method is called the *Tikhonov regularization method*. It will play a crucial part in the solution to the inverse problem. λ_1 and λ_2 are symmetric positive definite matrices that provide the flexibility of weighting the measurement and the forcing terms.

1.3. Derivation of the Dynamic Programming Equation

To minimize the least-squares error E in Eq. (6) over the sequence of the forcing vector, the dynamic programming method and *Bellman principle of optimality* are applied. This leads to defining the minimize value of E for any initial x and the number of stage n. Thus:

$$F_n \left(x \right) = \min_{f_i} E_n \left(x, f_i \right). \tag{7}$$

The recurrence formula can be derived by applying the *Bellman principle of optimality*:

$$F_{n-1} \left(x \right) = \min_{f_{n-1}} \left[\left(Qx_{n-1} - \hat{y}_{n-1} \right)^T \lambda_1 \left(Qx_{n-1} - \hat{y}_{n-1} \right) + \left(f_{n-1} \right)^T \lambda_2 \left(f_{n-1} \right) + F_n \left(Sx_{n-1} + Df_{n-1} \right) \right]. \tag{8}$$

This equation represents the classic dynamic programming structure in that the minimizing at any point is determined by selecting the decision f_{n-1} to minimize the immediate cost (first and second terms) and the remaining cost resulting from the decision (the third term). The solution is obtained by starting at the end of the process, $n = N$, and working backward toward $n = 1$. At the end point $n = N$, the minimum is determined from:

$$F_N \left(x \right) = \min_{f_N} \left[\left(Qx_N - \hat{y}_N \right)^T \times \lambda_1 \left(Qx_N - \hat{y}_N \right) + \left(f_N \right)^T \lambda_2 \left(f_N \right) \right]. \tag{9}$$

At this end point the minimum is obtained by choosing $f_N = 0$ which gives:

$$F_N \left(x \right) = \min_{f_N} [\left(Qx_N - \hat{y}_N \right)^T \lambda_1 \left(Qx_N - \hat{y}_N \right)]. \tag{10}$$

Eq. (10) can be expanded to:

$$F_N \left(x \right) = \left(x_N, Q^T \lambda_1 Q x_N \right) - 2 \left(x_N, Q^T \lambda_1 \hat{y}_N \right) + \left(\hat{y}_N, \lambda_1 \hat{y}_N \right). \tag{11}$$

Eq. (11) can be changed as:

$$F_N \left(x \right) = \left(x_N, R_N x_N \right) + \left(x_N, S_N \right) + q_N, \tag{12}$$

where:

$$R_N = Q^T \lambda_1 Q;$$

$$S_N = -2 Q^T \lambda_1 \hat{y}_N;$$

$$q_N = \left(\hat{y}_N, \lambda_1 \hat{y}_N \right).$$

Eq. (12) shows that F_N is quadratic in x_N. It can be proven inductively that all of the F_n are quadratic in x_n, thus for any n we can write:

$$F_n \left(x \right) = \left(x_n, R_n x_n \right) + \left(x_n, S_n \right) + q_n. \tag{13}$$

Substituting Eq. (13) into Eq. (8) and minimizing the equation, the optimal forcing term f_{n-1}^*:

$$\left(2\lambda_2 + 2D^T R_n D \right) f_{n-1}^* = -D^T S_n - 2D^T R_n S x_{n-1}. \tag{14}$$

For simplification the Eq. (14), let:

$$V_n = \left(2\lambda_2 + 2D^T R_n D \right)^{-1}; \tag{15}$$

$$H_n = 2D^T R_n. \tag{16}$$

Eq. (14) can now be written as:

$$f_{n-1}^* = -V_n D^T S_n - V_n H_n S x_{n-1}. \tag{17}$$

f_{n-1}^* is the identification wheel–rail force, which is the dynamic wheel–rail force caused by rail random irregularities without the weight reaction force. It is worth noting that, due to the limitation of accelerometers in low frequencies, the actual results of the wheel–rail vertical force is added by f_{n-1}^* and the weight reaction force.

These are recurrence formulas required to determine the optimal solution of Eq. (6).

1.4. Evaluation Method

Using *Pearson product-moment correlation coefficient* to measure the relationship between identification results and actual results, usually expressed by γ, with a range of [–1,+1]. The equation can be expressed by:

$$\gamma = \frac{\sum_{i=1}^{n} \left(F_{Si} - \overline{F}_S \right) \left(F_{Ii} - \overline{F}_I \right)}{\sqrt{\sum_{i=1}^{n} \left(F_{Si} - \overline{F}_S \right)^2} \sqrt{\sum_{i=1}^{n} \left(F_{Ii} - \overline{F} \right)^2}}, \tag{18}$$

where: F_{Si} is the SIMPACK simulation value in each

time point; F_{Ii} is the identification value in each time point; $\overline{F}_S$ is the standardization variables of the SIMPACK simulation value; $\overline{F}_I$ is the standardization variables of the identification value.

2. Laboratory Verification

First, a laboratory test is performed at TPL at Southwest Jiaotong University using the rolling and vibrating test-bed. The car body vertical acceleration, two bogie frames accelerations and four axle boxes accelerations are measured using DDS32 data acquisition system. Unfortunately, because of the limitation of test conditions, the rolling and vibrating test-bed can not measure the vertical and lateral interface forces directly. So we use a set of measured vertical acceleration response as inputs into the inverse vehicle model to identify other components of the vehicle acceleration responses, and compare with the measured results, by this way to verify the inversion mode.

Test scenario is shown in Fig. 1, the velocity of the rolling and vibrating test-bed is 250 km/h, the form of rail incentive is actual measured line spectrum of Wu–Guang line.

Using car body, two bogie frames and the first axle box (numbered from left to right) measured vertical acceleration as input into the inverse vehicle model, the fourth axle box acceleration response and the fourth wheel-set vertical force are identified (Figs 2 and 3).

From Fig. 2, the acceleration of the fourth axle box which identified by the inverse model is very similar to the measured value, and its correlation coefficient is 0.9756, which can be thought as height correlation. Fig. 3 shows the inversed vertical dynamic contact force for the fourth wheel-set, unfortunately, it is unable to be compared with measurement value due to the limitation of test-bed. It is worth noting that, due to the limitation of accelerometers in low frequencies, Fig. 3 is just the vertical dynamic contact force for the fourth wheel-set, the real vertical force should add the weight reaction force.

Fig. 1. Test scene of the rolling and vibrating test-bed

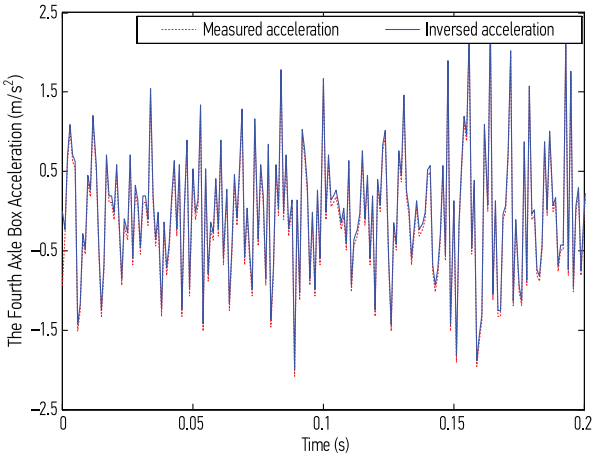

Fig. 2. Measured and inversed accelerations for the fourth axle box

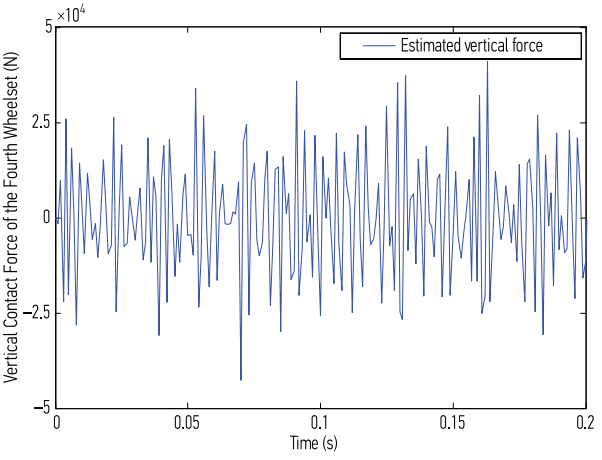

Fig. 3. The estimated vertical dynamic contact force for the fourth wheel-set

3. The Application of Inverse Model in High-Speed Train

For the railway vehicles, the wheel–rail dynamic contact will obviously increase in high-speed running state. Research shows that, when the train speed is increased from 80 km/h to 160 km/h and 250 km/h, between the wheel–rail dynamic force, P_1 (wheel–rail high frequency impact at the joint irregularity) increase by 45% and 100%, and P_2 (wheel–rail low frequency response force at the joint irregularity) increase by 38% and 80% (Zhai 2002).

Obviously, as the train speed increase, we must strive to reduce this dynamic force, thus avoid the increase of impact vibration and deterioration of wheel–rail contact in the high-speed railway. Therefore, it is necessary to strengthen the monitor dynamic force between wheel and rail in high speed operation. The paper uses the inverse method to identify the wheel–rail contact force of the vehicle in high-speed running condition, and thus provide the necessary reference for safe running.

The forces of interest are the forces Q and Y during railway vehicle movement, which are shown in Fig. 4.

The identification procedure is shown in Fig. 5.

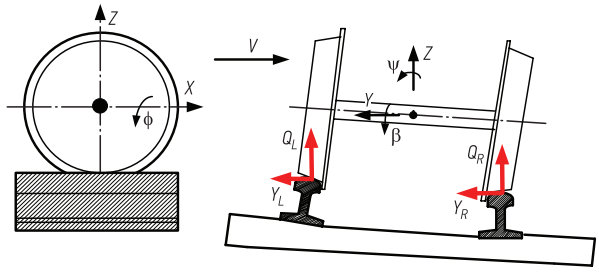

Fig. 4. Scheme for the contact forces for a wheel–rail system

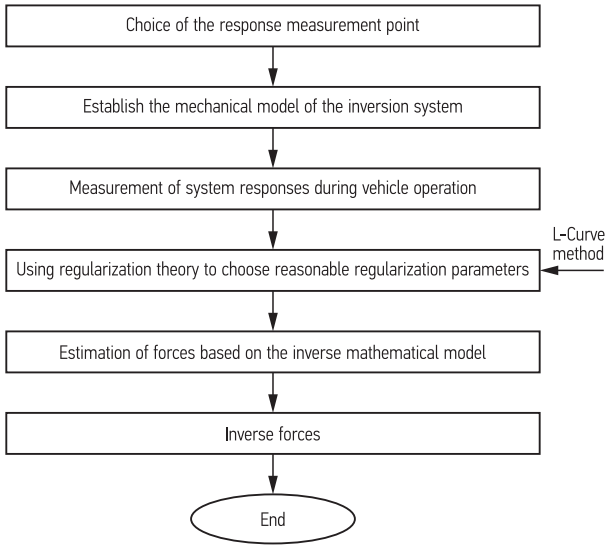

Fig. 5. Process of the proposed method for high-speed train's wheel–rail contact force

One kind of high-speed passenger vehicle which adopts two-axis bogies is chosen as an example. For describing this 7-rigid bodies system, 35 differential equations will be needed. Since there is only a weak coupling relation between the car's vertical motion and lateral motion, the vertical degree of freedom can be ignored when studying the car's lateral response and vice versa. Generally speaking, only some degrees of freedom such as vertical and pitch are taken into consideration when research vertical response; and lateral, roll and yaw movement are taken into consideration when study lateral response. For simplifying the research of the wheel–rail contact force, the research of identifications of vertical contact force and lateral contact force will be separated. The degrees of freedom considered for vehicle system's vertical random vibration study and lateral random vibration study are listed respectively in Tables 1 and 2.

In view of the cost of experiment and the limitation of the data from the experiment, one vehicle dynamic model is built by SIMPACK, which is a multibody analysis software widely used in the railway industry. Choosing actual measured track irregularity of Beijing-Tianjin high speed train line as input, a kinetic simulation of high-speed vehicle at the speed of 250 km/h is performed. In order to make the results of SIMPACK

Table 1. The degrees of freedom in the vertical random vibration

Component	DOF						No. of items	No. of DOF
	X	Y	Z	Φ	Ψ	β		
Car body	×	×	√	×	√	×	1	2
Bogie	×	×	√	×	√	×	2	4
Wheel-set	×	×	√	×	×	×	4	4
Total DOF								10

Note: *X*, *Y*, *Z*, Φ, Ψ and β indicate the longitudinal, lateral, vertical, roll, pitch and yaw for car body, bogie and wheel-set, respectively.

Table 2. The degrees of freedom in the lateral random vibration

Component	DOF						No. of items	No. of DOF
	X	Y	Z	Φ	Ψ	β		
Car body	×	√	×	√	×	√	1	3
Bogie	×	√	×	√	×	√	2	6
Wheel-set	×	√	×	×	×	√	4	8
Total DOF								17

Note: *X*, *Y*, *Z*, Φ, Ψ and β indicate the longitudinal, lateral, vertical, roll, pitch and yaw for car body, bogie and wheel-set, respectively.

simulation replace a practical real vehicle test, the vehicle model developed in SIMPACK is a very refined model using the nonlinear wheel–rail contact geometry, nonlinearities between creep sliding rate and creep force, and the nonlinear suspension elements and links in the vehicle system. Contrast verification has been conducted between the result of simulation and the result of real test which ensures that the real line test can be substituted by the simulation to some extent. The simulation model can then be used with some confidence to calculate wheel contact forces. By choosing the responses that gotten in SIMPACK, from some special parts (such as vertical, lateral and longitudinal accelerations of axle box) as the input for plugging into the inverse mathematical model, inverse solutions as lateral and vertical forces of wheel–rail and derailment coefficient can be worked out. Then, all these results are taken into comparison with the results of SIMPACK simulation in order to prove the availability of inversion mathematical model.

SIMPACK model is displayed in Fig. 6. The dynamic parameters of vehicle system are listed in Appendix A and Appendix B (Ma *et al.* 2010).

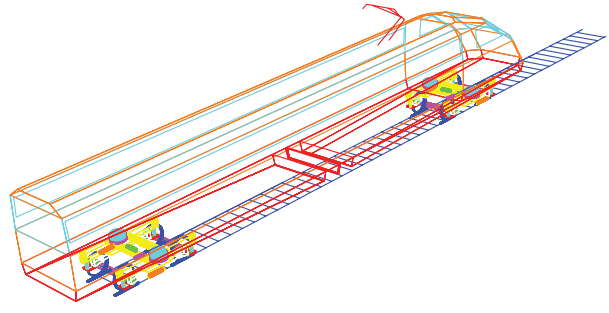

Fig. 6. The vehicle dynamics model

3.1. Wheel–Rail Vertical and Lateral Forces Inversion at the Speed of 250 km/h

Taking the track irregularity of Beijing–Tianjin high speed train line as input, the running speed for simulated is 250 km/h. Then, choosing the vertical and lateral accelerations of axle box which are gotten from the dynamics simulation as the input responses of inverse mathematical model, inverse solution of wheel–rail forces are finally calculated by MATLAB. Figs 7 and 8 show the wheel–rail vertical and lateral contact forces comparison of the results between the inverse results and SIMPACK simulation results for the first wheel-set (direction of the forward motion).

With the comparison of Fig. 7, the peak values of inversed vertical forces are always smaller than simulated ones. It may be caused by neglecting of the dampers by choosing the acceleration of axle box as input which cannot offer sufficient information for the inversion model. But in terms of tendency, the inversed result and the simulated result are accordant, and in time domain, its correlation coefficient is 0.7856, which can be thought as significant correlation. From Fig. 8, the peak values of inversed lateral forces are also similar to simulated ones, and in time domain, its correlation coefficient is 0.6984, which can also be thought as significant correlation. From the view of time domain correlation coefficient, the lateral wheel–rail force prediction is worse than the vertical, which is caused by strong non-linear factors of vehicles in the lateral.

PSD (Power spectral density) analysis result from Fig. 9 show that, for vertical and lateral inverse results, both in low frequency range and in high frequency range in [0, 100] Hz, the PSD of the inverse forces are as the same as the simulation results. This shows that the inverse mathematical model can predict good result for the high-speed train wheel–rail vertical and lateral forces.

3.2. Comparison of Derailment Index at the Speed of 250 km/h

Wheel-set derailment index, a coefficient that describes vehicle's performance against derailment, comprehensively reflects the lateral and vertical wheel–rail forces' variations. Under the speed of 250 km/h, the derailment index which is gotten from the inverse model and the SIMPACK simulation is compared. It is shown in Fig. 10.

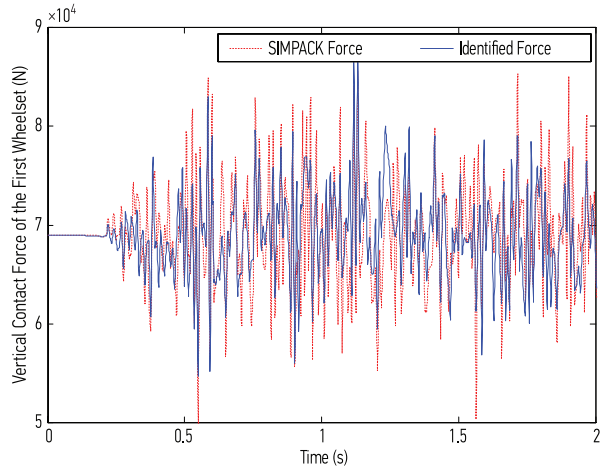

Fig. 7. Vertical wheel–rail contact force comparison for first wheel-set

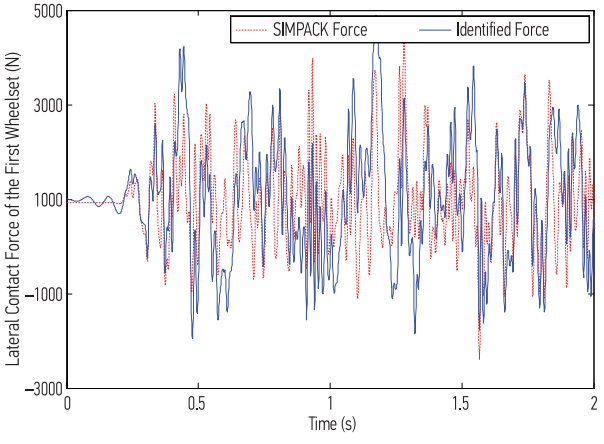

Fig. 8. Lateral wheel–rail contact force comparison for first wheel-set

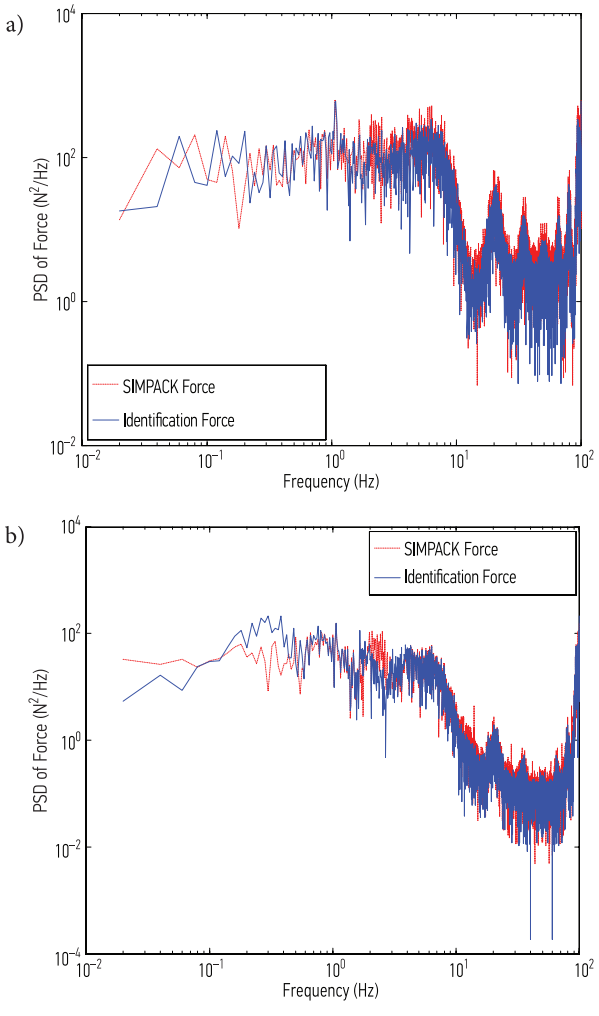

Fig. 9. PSD of vertical (a) and lateral (b) contact force for first wheel-set

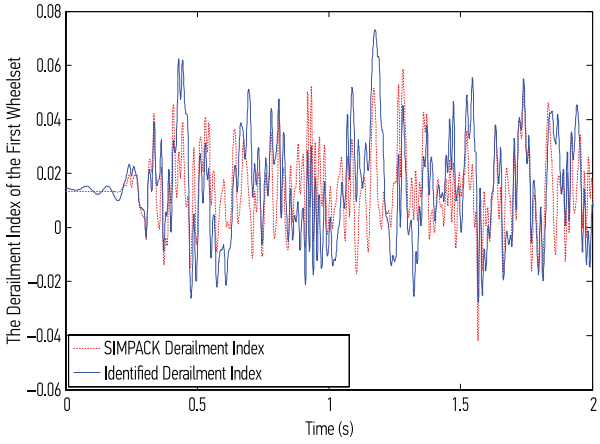

Fig. 10. Comparison of index coefficient for first wheel-set

By comparing the derailment index, it can be found that the tendencies of the results are quite accordant. It shows that the inversion mathematical model is a good tool to predict vehicle's derailment index, thus can play an important role in vehicle's real time detection.

Conclusion

The purpose of this article is to put forward an effective inversion mathematical model which can be used to inverse the wheel–rail contact force and the vibration response of high-speed passenger vehicle. Considering the difficulties in validating without direct measurements the results from the rolling and vibration test-bed and SIMPACK simulation are quite encouraging.

The main conclusions:

1. Bellman principle of optimality which makes the identified results only be relevant to the responses of current and adjacent moments measured results, and irrelevant to the past responses and inverse results. The method effectively avoid the accumulative errors and transfer errors, enhance the numerical stability.
2. Inversion model is imported to identify the wheel–rail contact forces of high-speed passenger vehicle. The experiment data of the laboratory test are used to verify the inversion model. Using some parts of measured accelerations to identify the other component of accelerations, and compare with laboratory tests. The results show that the inversion model can be used to identify the unknown output responses for interesting places.
3. Using SIMPACK model simulation which is verified by the field validation, accelerations of three directions of axle box are then chosen with some confidence as input of inversion model and success to identify and detect wheel–rail force.
4. From the time domain and frequency domain, the comparison of the results between inverse and SIMPACK models are given. The results show that, the inverse mathematical model has high relatively precision for inversing the wheel–rail contact forces of operation high-speed vehicle. And in time domain, their correlation coefficients are greater than 0.5, can be thought as significant correlation. PSD analysis shows that, both in low frequency range and in the high frequency range, the PSD of the inverse forces are as the same as the simulation results. In general, the inversion model has a high precision for inversing the wheel–rail forces of high-speed vehicle and can reflect precisely the time-dependent variation of wheel–rail contact forces. This method enables vehicle's security real time protection.

The model is applicable in the range of linearity. In cause of considering the nonlinearity of wheel–rail contact, the inversion model will be modified in order to get a more precise solution. In addition, the regret is that the verification of the model's accuracy merely rest on the laboratory test and SIMPACK simulation. The next step will consider the field test which is not included in this article yet.

Acknowledgments

This research was supported in part by National Key Technology R&D Program in the 11th Five year Plan of China (2009BAG12A04-A11); The National Natural Science Foundation of China (51005190); The Fok Ying Tong Education Foundation (Grant No. 122014); University Doctor Academics Particularly Science Research Fund (SWJTU09ZT23) and also was supported by the Scientific Research Foundation of Graduate School of Southwest Jiaotong University.

References

Dobson, B. J.; Rider, E. 1990. A review of the indirect calculation of excitation forces from measured structural response data, *Proceedings of the Institution of Mechanical Engineers, Part C: Journal of Mechanical Engineering Science* 204(2): 69–75. http://dx.doi.org/10.1243/PIME_PROC_1990_204_080_02

Esveld, C. 2001. *Modern Railway Track*. MRT-Productions. 632 p.

Giergiel, J.; Uhl, T. 1989a. Identification of impact forces in mechanical systems, *Archives of Machine Design* 36(2–3): 321–336.

Giergiel, J.; Uhl, T. 1989b. Identification of the input excitation forces in mechanical structures, *Archives of Transport* 1(1): 8–24.

Hansel, E. 1991. *Inverse Theory and Applications for Engineers*. Prentice Hall. 352 p.

Kammer, D. C. 1998. Input force reconstruction using a time domain technique, *Journal of Vibration and Acoustics* 120(4): 868–874. http://dx.doi.org/10.1115/1.2893913

Law, S. S.; Chan, T. H. T.; Zeng Q. H. 1997. Moving force identification: a time domain method, *Journal of Sound and Vibration* 201(1): 1–22. http://dx.doi.org/10.1006/jsvi.1996.0774

Ma, W.; Luo, S.; Song, R. 2010. Influence of the orientation stiffness of tumbler journal box to the stability of high speed vehicles, in *2010 International Conference on Computer Design and Applications (ICCDA 2010)*, 25–27 June, 2010, Qinhuangdao, Hebei, China, Vol. 3, 282–286. http://dx.doi.org/10.1109/ICCDA.2010.5540811

Nordström, L. J. L.; Nordberg, T. P. 2002. A critical comparison of time domain load identification methods, in *Proceedings:*

the Sixth International Conference on Motion and Vibration Control, August 19–23, 2002, Saitama, Japan, Vol. 2, 1151–1156.

Ronasi, H.; Johansson, H.; Larsson, F. 2009. A numerical framework for load identification with application to wheel-rail contact forces, in *ECCOMAS International Symposium IPM 2009 on Inverse Problems in Mechanics of Structure and Materials*, April 23–25, 2009, Rzeszów–Łańcut, Poland, 69–70.

Stevens, K. K. 1987. Force identification problems: an overview, in *Proceedings of the 1987 SEM Spring Conference on Experimental Mechanics*, June 14–19, 1987, Houston, Texas, 838–844.

Uhl, T. 2007. The inverse identification problem and its technical application, *Archive of Applied Mechanics* 77(5): 325–337. http://dx.doi.org/10.1007/s00419-006-0086-9

Uhl, T.; Pieczara, J. 2003. Identification of operational loading forces for mechanical structures, *Archives of Transport* 15(2): 109–126.

Xia, F.; Cole, C.; Wolfs, P. 2008. Grey box-based inverse wagon model to predict wheel–rail contact forces from measured wagon body responses, *Vehicle System Dynamics* 46(1): 469–479. http://dx.doi.org/10.1080/00423110801993102

Zhai, W. M. 2002. *Vehicle-Track Coupling Dynamics*. China Railway Publishing House, Beijing (in Chinese).

Zhu, T.; Xiao, S.-N.; Yang, G.-W. 2011. State-of-the-art development of load identification and its application in study on wheel-rail forces, *Journal of the China Railway Society* 33(10): 29–36 (in Chinese).

APPENDIX A

The dynamic parameters of the vehicle system

Parameters	Value
Car body mass	38936 kg
Bogie frame mass	4172 kg
Wheel-set mass	1627 kg
Length between truck pivot centers	17.375 m
Wheel base	2.5 m
Height of C.G. above rail for car-body	2.134 m
Height of C.G. above rail for framework	0.96 m
Roll moment of inertia of car body	96100 kg·m^2
Pitch moment of inertia of car body	1.67E6 kg·m^2
Yaw moment of inertia of car body	1.7E6 kg·m^2
Roll moment of inertia of bogie frame	2110 kg·m^2
pitch moment of inertia of bogie frame	2602 kg·m^2
Yaw moment of inertia of bogie frame	4080 kg·m^2
Roll moment of inertia of wheel-set	818 kg·m^2
pitch moment of inertia of wheel-set	145 kg·m^2
Yaw moment of inertia of wheel-set	822 kg·m^2
Longitudinal stiffness of primary suspension (every axle box)	1.21E8 N/m
Lateral stiffness of primary suspension (every axle box)	1.34E7 N/m
Vertical stiffness of primary suspension (every axle box)	7.5E5 N/m
Damp of primary vertical damper	10000 N·s/m
Longitudinal stiffness of secondary suspension	1.33E5 N/m
Lateral stiffness of secondary suspension	1.33E5 N/m
Vertical stiffness of secondary suspension	2.03E5 N/m
Damp of secondary vertical damper	5000 N·s/m
Damp of secondary lateral damper	15000 N·s/m

APPENDIX B

Nomenclature

M	system mass matrix
C	system damping matrix
K	system stiffness matrix
F	vector of the input excitation forces
$\ddot{X}(t)$	acceleration vector
$\dot{X}(t)$	velocity vector
X(t)	displacement vector
S	exponential matrix
D	input influence matrix
Q	selection matrix
E	least-squares error of the solution
T	the transpose of a matrix
y_i	output variables of the identification formula
$\hat{y}_i$	output variables of the measurement formula
λ_1	weighting matrix
λ_2	Tikhonov regularization parameter
f^*_{n-1}	the (n–1)th vertical and lateral forces
γ	correlation coefficient
F_{Si}	the SIMPACK simulation value
F_{Ii}	the identification value
$\overline{F}_S$	the standardization variables of the SIMPACK simulation value
$\overline{F}_I$	the standardization variables of the identification value
P_1	wheel–rail high frequency impact at the joint irregularity
P_2	wheel–rail low frequency response force at the joint irregularity
$Q_{(R,L)}$	the right and left vertical wheel–rail force
$Y_{(R,L)}$	the right and left lateral wheel–rail force
X	the longitudinal of car body, bogie and wheel-set
Y	the lateral of car body, bogie and wheel-set
Z	the vertical of car body, bogie and wheel-set
Φ	the roll of car body
Ψ	the pitch of car body
β	the yaw of car body